VERTICAL GROUND MOTION: CHARACTERISTICS, RELATIONSHIP WITH HORIZONTAL COMPONENT, AND BUILDING-CODE IMPLICATIONS

Y. Bozorgnia[1], K.W. Campbell[2], and M. Niazi[3]

ABSTRACT

In this study, the characteristics of peak vertical ground acceleration and vertical response spectra are examined and the differences between the vertical and horizontal components are investigated. This was accomplished with a comprehensive database of 2,823 free-field components (three per recording) of uncorrected peak ground acceleration from 48 worldwide earthquakes and 1,308 free-field components of corrected peak ground acceleration and response spectral acceleration from 33 worldwide earthquakes, all recorded within 60 km of the causative fault from earthquakes ranging from 4.7 to 7.7 in magnitude. Peak and spectral acceleration attenuation models were developed for both the vertical and horizontal components as a function of magnitude, source-to-site distance, type of faulting, and local soil conditions. An analysis of residuals indicated that the vertical-to-horizontal (V/H) spectral ratios predicted by these attenuation relationships show no significant bias with respect to observed V/H and the modeled parameters. The study clearly demonstrates the strong dependence of V/H on oscillator period, source-to-site distance, and local soil conditions. V/H shows a weaker and more limited dependence on magnitude and type of faulting. The largest short-period V/H ratios are observed to occur on Holocene Soil at short periods and short distances where they can reach values in excess of 1.5 at 0.1-sec period. The largest long-period V/H ratios are observed to occur on Hard Rock where they can reach values as high as 0.7. Generally V/H is 0.5 or less at the longer periods (0.3 to 2.0 sec). We conclude that the standard engineering practice of assigning V/H a value of two-thirds is unconservative at short periods, especially for unconsolidated soil, but conservative at long periods, and should be modified. We propose a simplified model for estimating a design vertical response spectrum for engineering purposes from a simplified model of V/H that better fits the observed trends in V/H. The procedure seems to have merit and will be refined in a future study.

INTRODUCTION

Previous studies of recorded free-field ground motion have revealed that the vertical component is generally richer in high-frequency energy than the horizontal component and its amplitude at these frequencies can exceed that of the horizontal component. These differences are especially evident in vertical and horizontal response spectra from recordings located close to the causative fault.

Niazi and Bozorgnia (1989, 1990, 1991, 1992) analyzed over 700 horizontal and vertical response spectra from 12 earthquakes recorded by the SMART-1 strong-motion array in Taiwan. In subsequent studies, Bozorgnia and Niazi (1993) examined 159 horizontal and vertical

[1] Managing Engineer, Exponent Failure Analysis Associates, Menlo Park, California
[2] Vice President, EQE International, Inc., Evergreen, Colorado
[3] Principal, Berkeley Geophysical Consultants, Berkeley, California

response spectra from the 1989 Loma Prieta, California, earthquake and Bozorgnia and others (1995) analyzed 123 horizontal and vertical response spectra of 41 soil sites from the Northridge, California, earthquake. Ansary and Yamazaki (1998) analyzed 2,166 horizontal and vertical response spectra from 387 earthquakes recorded at 76 Japan Meteorological Agency (JMA) sites in Japan. All of these investigators came to the same conclusion: that the vertical-to-horizontal (V/H) spectral ratio of strong ground motion is a strong function of oscillator period with short periods having higher ratios than long periods. They also found that V/H spectral ratios are only weakly correlated with magnitude, especially beyond the immediate vicinity of the fault. Those studies that looked at near-source recordings additionally found that V/H ratios of peak ground acceleration and response spectra were also a strong function of source-to-site distance and could approach or exceed a value of 1.0 at short periods.

Several investigators have developed attenuation relationships for both horizontal and vertical components of strong ground motion (e.g., Campbell, 1982; Abrahamson and Litehiser, 1989; Sadigh and others, 1993; Abrahamson and Silva, 1997; Campbell, 1997; Ansary and Yamazaki, 1998). Predicted accelerations and response spectra from these attenuation relationships confirm the above conclusions regarding the V/H ratio. Amirbekian and Bolt (1998) have also examined the differences between the spectral characteristics of near-source vertical and horizontal ground motions from a seismological point of view. They concluded that the high-amplitude, high-frequency vertical accelerations that are observed on near-source accelerograms are most likely generated by the conversion of shear waves to compressional waves (S-to-P conversion) within the transition zone between the underlying bedrock and the overlying softer sedimentary layers.

The main objective of this study was to identify the general characteristics and differences of vertical and horizontal response spectra in terms of some fundamental properties of the earthquakes and stations that recorded them. These properties include earthquake magnitude, source-to-site distance, type of faulting, and local soil conditions. This objective was accomplished by analyzing near-source ground motions of numerous worldwide earthquakes. The specific tasks involved in accomplishing this objective were as follows:

1. We compiled a comprehensive database of near-source vertical and horizontal time histories and response spectra, building on our previous study of the horizontal component of peak ground acceleration (Campbell and Bozorgnia, 1994; Campbell, 1997).
2. We used the compiled database to develop attenuation relationships for the vertical and horizontal components of peak ground acceleration and acceleration response spectra taking into account the effects of magnitude, distance to the causative fault, type of faulting, and local soil conditions.
3. We used the vertical and horizontal attenuation relationships to examine and evaluate the differences between the spectral characteristics of the vertical and horizontal ground motions and to propose a model for estimating V/H.
4. We used the observed and modeled characteristics of V/H to evaluate two simplified procedures for developing a vertical response spectrum from a horizontal response spectrum for practical engineering and building-code applications by (a) shifting the horizontal response spectrum to shorter periods and adjusting its amplitude or (b) applying a simplified V/H spectral ratio to the horizontal spectrum.

STRONG-MOTION DATABASE

This study utilized a comprehensive worldwide database of near-source accelerograms that were recorded between 1957 and 1995. The database is an expanded and updated version of the one that was used by two of the authors to develop a near-source attenuation relationship for peak horizontal acceleration (Campbell and Bozorgnia, 1994; Campbell, 1997). It was expanded to include response spectral ordinates and significant earthquakes that have occurred since 1992 (Table 1). The strong-motion parameters analyzed in this study include uncorrected peak ground acceleration (Uncorrected PGA), corrected peak ground acceleration (Corrected PGA), and 15 components of 5%-damped response spectral acceleration (SA) at natural oscillator periods of 0.04, 0.05, 0.075, 0.1, 0.15, 0.2, 0.3, 0.4, 0.5, 0.75, 1.0, 1.5, 2.0, 3.0, and 4.0 sec. The terms "Uncorrected" and "Corrected" refer to the standard levels of accelerogram processing referred to as Phases 1 and 2. Uncorrected PGA is measured directly from the accelerogram or, if the accelerogram has been processed, from the baseline and instrument corrected acceleration record. Corrected PGA is measured from the acceleration record after it has been band-passed filtered and decimated to a uniform time interval.

The database of Uncorrected PGA includes 941 near-source recordings, each having two horizontal and one vertical component (2,823 individual components altogether) from 48 worldwide earthquakes ranging from 4.7 to 7.7 in magnitude. This corresponds to a 50% increase in the number of Uncorrected PGA values that had been used in our previous study. The database of Corrected PGA and SA consists of 436 near-source recordings (1,308 individual components) from 33 worldwide earthquakes ranging from 4.7 to 7.7 in magnitude. It is important to note that the Uncorrected database has over double the number of recordings as the Corrected database. The importance of this difference on the regression results will become evident later in the paper. The distribution of these recordings with respect to magnitude and distance is given in Figure 1.

All of the earthquakes occurred in a shallow crustal tectonic environment. All of the recordings are considered to be free field, defined as ground level of an instrument shelter or a building less than three stories high (less than seven stories high if located on Hard Rock). Recordings on dam abutments were included to enhance the database of rock recordings. Recordings obtained in the basements of buildings of any size or at the toe or base of a dam were excluded.

The magnitude measure used to characterize the size of an earthquake is moment magnitude (M_W). The distance measure is defined as the shortest distance from the area of seismogenic rupture on the causative fault to the recording site, hereafter referred to as distance to seismogenic rupture (R_S). R_S was restricted to 60 km or less to avoid the complicating problems related to the arrival of multiple reflections from the lower crust, as was clearly observed during the 1989 Loma Prieta earthquake (Somerville and Yoshimura, 1990; Campbell, 1991). This distance range is believed to include most ground shaking of engineering interest, except for possibly long-period spectral accelerations on extremely poor soil.

The types of faulting were classified into three categories defined as Strike Slip, Reverse, and Thrust. The Strike Slip faulting category includes primarily vertical or near-vertical faults with predominantly lateral slip. The Reverse category includes steeply dipping faults with either predominantly reverse slip or nearly equal amounts of reverse and lateral slip (reverse-oblique slip). The Thrust category includes shallow dipping faults with predominantly thrust mechanisms. The last category includes blind-thrust events such as the 1983 Coalinga, 1987

Whittier Narrows, and 1994 Northridge earthquakes. Since there is only one normal-faulting event in the database, this earthquake was placed in the Strike Slip category. There are 20 Strike Slip, 7 Reverse, and 6 Thrust events in the Corrected database.

Local soil conditions were classified into four categories defined as Holocene Soil, Pleistocene Soil, Soft Rock, and Hard Rock. The Holocene Soil category includes soil deposits of Holocene age (11,000 years or less) generally described on geologic maps as recent alluvium. The Pleistocene Soil category includes soil deposits of Pleistocene age (11,000 to 1.5 million years) generally described on geologic maps as older alluvium and terrace deposits. The Soft Rock category primarily includes sedimentary rock deposits of Tertiary age (1.5 to 100 million years). The Hard Rock category primarily includes older sedimentary rock deposits, metamorphic rock, and crystalline rock. There are 239 Holocene Soil, 84 Pleistocene Soil, 61 Soft Rock, and 52 Hard Rock recordings in the Corrected database.

REGRESSION ANALYSIS

An initial attempt at developing an attenuation relationship directly in terms of the V/H ratio failed. The relationship between V/H and magnitude, source-to-site distance, type of faulting, and local soil conditions was too complicated to model independently. Instead, we decided to develop a consistent set of attenuation relationships for the horizontal and vertical components of PGA and SA and use these to estimate V/H. This approach was later validated from an analysis of residuals.

After considerable exploratory analysis, the following equation was finally selected to represent the attenuation of PGA and SA for both horizontal and vertical components:

$$\begin{aligned} \ln Y = {} & c_1 + c_2 M_W + c_3 (8.5 - M_W)^2 + c_4 \ln (\{R_S^2 + [(c_5 S_{HS} + c_6 \{S_{PS} + S_{SR}\} + c_7 S_{HR}) \\ & \exp (c_8 M_W + c_9 \{8.5 - M_W\}^2)]^2\}^{1/2}) + c_{10} F_{SS} + c_{11} F_{RV} + c_{12} F_{TH} \\ & + c_{13} S_{HS} + c_{14} S_{PS} + c_{15} S_{SR} + c_{16} S_{HR} \end{aligned} \quad (1)$$

where Y is either the vertical component (Y_V) or the geometric average of the two horizontal components (Y_H) of PGA or SA in g (g = 981 cm/sec^2); M_W is moment magnitude, R_S is the distance to seismogenic rupture in km; S_{HS} = 1 for Holocene Soil, S_{PS} = 1 for Pleistocene Soil, S_{SR} = 1 for Soft Rock, S_{HR} = 1 for Hard Rock, and $S_{HS} = S_{PS} = S_{SR} = S_{HR} = 0$ otherwise; F_{SS} = 1 for Strike Slip faulting, F_{RV} = 1 for Reverse faulting, F_{TH} = 1 for Thrust faulting, and $F_{SS} = F_{RV} = F_{TH} = 0$ otherwise; and c_1 through c_{16} are regression coefficients.

The exponential magnitude term on the second line of Equation (1) accounts for the magnitude dependence of Y as a function of distance. After some preliminary analyses, we determined that the coefficients in this term should be set so that Y is independent of M_W at $R_S = 0$, referred to as magnitude saturation. It is equivalent to setting $c_8 = -c_2/c_4$ and $c_9 = -c_3/c_4$. The coefficients c_5 through c_7 determine the degree of distance saturation of Y for a given magnitude. As modeled, differences in these coefficients will allow the value of Y between different soil categories to vary with distance, permitting the possibility of nonlinear soil behavior.

The regression analysis was performed using the generalized nonlinear regression module in SYSTAT, a commercially available statistical analysis software package offered by SPSS, Inc. of Chicago, Illinois. The loss function used in the analysis was ordinary least squares. As in our previous study, no weights were applied during the analysis because we believed that the distribution of Uncorrected recordings with respect to magnitude and distance was not

significantly biased. However, inspection of Figure 1 indicates that this is not necessarily true for the Corrected database. The use of weights or a similar procedure, such as two-step or random-effects regression, will be explored in a future study.

When all of the coefficients were allowed to be freely determined during the regression analysis, the analysis commonly became unstable. This was due mainly to the tradeoff between c_2 through c_7 during the regression (recall that c_8 and c_9 were constrained). To make the regression more stable, c_2 was set equal to the value determined from the better-constrained analysis of Uncorrected PGA.

We found that there was a considerable degree of period-to-period variability in the regression coefficients that caused the predicted spectra to be very jagged near the limits of the magnitude and distance ranges. In order to reduce this jaggedness to an acceptable degree, some of the coefficients were smoothed. In order to make the spectra completely smooth at all magnitudes and distances, the coefficient smoothing would have to be done iteratively over the entire period range. We believed that this more rigorous smoothing process was not necessary to meet the objectives of the current study. Methods for producing smoothed response spectra suitable for design will be explored in a future study. The partially smoothed regression coefficients for the horizontal and vertical components of PGA and SA that were used in the present study of V/H are listed in Table 2. Because of the extremely small number of 0.04-sec SA values, no amount of smoothing could bring it into line. Therefore, this spectral ordinate was removed from the analysis.

The difference in the regression results for the horizontal component of Uncorrected and Corrected PGA is demonstrated in Table 2 and in Figure 1. Figure 1 indicates that this difference is largest at short distances and small magnitudes where there are fewer recordings. Similar differences are observed for the vertical component (not shown). The plots of the normalized residuals clearly show the narrower magnitude range for the Corrected data. The residuals, which represent the difference between the observed and predicted values of ln Y, were normalized by dividing them by the standard error of the Uncorrected PGA regression analysis. In this way one can visually compare the scatter in the residuals on a consistent basis. The residual plots together with the standard errors and r^2 values (goodness of fit) in Table 2 indicate that both the Uncorrected and Corrected PGA fits are equally good, given their respective databases. The differences are principally the result of the bias in the number and distribution of recordings in the Corrected database.

Figures 2 and 3 show how the predicted horizontal and vertical response spectra scale with magnitude, distance, local soil conditions, and type of faulting. The horizontal spectra clearly show a trend towards increasing predominate period with increasing magnitude. This trend is largely missing in the vertical spectra. The dependence of predominant period on distance for both the vertical and horizontal spectra is negligible, except possibly at 60 km. It should also be noted that the predominate periods of the horizontal spectra (0.2 to 0.5 sec) are longer than those of the vertical spectra (around 0.1 sec).

The behavior of SA with soil conditions is also significantly different between the horizontal and vertical spectra. The horizontal spectra show relatively little difference between the different soil categories at short periods for the distance shown (R_S = 10 km). However, the horizontal Hard Rock spectrum is much smaller than that of the other soil categories at longer periods. The vertical spectra, on the other hand, are all quite similar for the different soil categories, except for

the larger amplitude for Holocene Soil at short periods. Both the horizontal and vertical spectra show the same tendency towards higher amplitudes for Reverse and Thrust faulting at short and moderate periods. At periods greater than about 1.0 sec, however, these differences become negligible. This trend of decreasing difference in SA with increasing period for different types of faulting is consistent with the expected effects of dynamic stress drop and the expectation that Reverse and Thrust faulting is generally associated with higher stress drops.

V/H RATIO

The horizontal and vertical regression results can be used to derive an attenuation relationship for V/H by subtracting the logarithm of the vertical and horizontal components of Y calculated from Equation (1), giving:

$$\ln V/H = \ln Y_V - \ln Y_H \qquad (2)$$

The plots of the normalized residuals of ln V/H versus magnitude and distance shown in Figures 4 and 5 demonstrate the validity of Equation (2) as an unbiased predictor of V/H. Note, however, that the difference between the values of V/H using the Corrected and Uncorrected databases can be as much as 20%, more than for horizontal and vertical SA. Other plots (not shown) clearly confirm that the prediction of V/H from Equation (2) is equally unbiased with respect to SA at other periods, types of faulting, and soil categories. The bias and standard errors derived from these residuals are listed in Table 3. Note that the standard errors are somewhat smaller than those from the horizontal regression.

To further verify the validity of Equation (2), we compared the standard errors and scaling characteristics derived from this equation with those determined from our preliminary regression on V/H. Although the regression results for V/H were erratic, they did confirm that Equation (2) fit the observed values of V/H just as well as a model derived from a direct regression on ln V/H.

Figure 6 demonstrates the attenuation characteristics of V/H for Strike Slip faulting and Holocene Soil. This figure clearly shows that V/H attenuates rather steeply with distance at short periods, but that this rate decreases with increasing period until at periods between 0.3 and 1.0sec V/H begins to increase with distance. As subsequent plots will show, this transition from decreasing to increasing V/H with distance actually occurs between 0.3 and 0.4 sec. V/H scaling with magnitude also decreases with distance, becoming insignificant at 0.3 sec. On these and subsequent plots, horizontal lines are plotted at V/H = 0.5, 0.67, and 1.0 for reference.

Figures 7 and 8 demonstrate the effect of soil conditions on V/H as a function of magnitude and distance, respectively. Also shown on Figure 7 is the effect of fault type. The effect of the type of faulting was found to be independent of magnitude, distance, and soil conditions, so this effect can be shown on a single plot. Only at very short and very long periods is V/H different for the three faulting categories. At short periods, Strike Slip faulting has higher V/H but differences between Reverse and Thrust faulting are barely distinguishable. The differences at long periods might not be significant, since there are fewer recordings at these periods. Soil effects are most pronounced for Holocene Soil (at short periods) and Hard Rock (at long periods). The difference in Holocene Soil diminishes with decreasing magnitude and increasing distance, however, the difference in Hard Rock remains relatively constant at all magnitudes and distances. At small magnitudes and large distances, the only effect of local soil conditions that remains is higher V/H on Hard Rock a periods exceeding about 0.2 sec.

The dependence of V/H on magnitude and distance for each of the soil categories are better demonstrated in Figures 9 and 10, respectively. The effect of magnitude (shown for R_S = 10 km) is most significant for Holocene Soil at periods shorter than 0.3 sec. The other soil categories show very little magnitude scaling and what scaling exists becomes negligible at larger distances. The effect of distance is also most pronounced for Holocene Soil, but the other soil categories show significant scaling at longer periods where V/H increases with distance. Once a distance of 60 km is reached, most of the dependence of V/H on distance at short periods has ended but differences at longer periods remain significant.

SIMPLIFIED VERTICAL SPECTRUM

For practical engineering applications, and especially when vertical response spectra are not available, it is desirable to develop a vertical response spectrum from an approximate relationship between the vertical and horizontal spectrum. In this section, we examine two such simplified methods.

The first method is to shift the horizontal spectrum to shorter periods and then reduce its amplitude to approximate the vertical spectrum. The method was proposed by Watabe and others (1990) and later evaluated by Bozorgnia and others (1996). Shifting the horizontal spectrum to shorter periods is consistent with the fact that vertical ground motion is richer in high-frequency energy than horizontal ground motion. Based on the observed differences between the spectral content of vertical and horizontal spectra for the 1994 Northridge earthquake, Bozorgnia and others (1996) suggested a period shift factor of 2.0. Amirbekian and Bolt (1998) also found an approximate ratio of 2.0 between the vertical and horizontal values of the spectral corner frequency f_{max}.

Based on these past studies, we examine the following simplified procedure for estimating a vertical spectrum from a horizontal spectrum: (1) shift the horizontal acceleration spectrum to a shorter period by dividing each period by a factor of 2.0, and (2) reduce the spectral ordinates of the shifted horizontal spectrum by the V/H ratio of PGA. It should be noted that the PGA ratio is a function of source-to-site distance. Figure 11 shows the results of applying this simplified procedure. The agreement between the predicted and shifted spectra is reasonably good at M_W 6.5 for Holocene Soil and at M_W 7.5 for Hard Rock. However, the same level of agreement is not achieved for other magnitudes and soil categories. This simplified method is, therefore, limited in its usefulness. A more general agreement between the predicted and shifted horizontal spectrum might be possible if a variable period shift is used. This latter approach will be explored in a future study.

The second method is to apply a simplified V/H spectral ratio to the horizontal spectrum. As previously discussed, the V/H spectral ratio is a strong function of period, source-to-site distance, and local soil conditions, and more weakly dependent on magnitude and type of faulting. However, for practical engineering applications it is desirable to model only those factors that have the greatest influence on the V/H and make conservative assumptions regarding the influence of the other factors. Figure 12 shows our attempt at defining a simplified model for estimating V/H. Since the behavior of the observed V/H spectral ratio with distance is much different for Holocene Soil than for the other three soil categories, a separate model is proposed for this category. The dependence of V/H on distance is generally similar for Pleistocene Soil, Soft Rock, and Hard Rock, but less than that for Holocene Soil. Figure 12 also shows the

comparison between the simplified V/H spectral model and predicted V/H for different magnitudes and soil conditions. For Holocene Soil, the proposed V/H ratio of 0.5 is relatively conservative at mid periods and can, therefore, be extended to periods longer than 1.0 sec. However, for the other three soil categories, the predicted V/H ratio is greater than 0.5 beyond 1.0 sec, approaching a value of 0.7 at about 4.0 sec.

BUILDING-CODE APPLICATION

In this section we evaluate the definition of vertical ground motion in the 1997 Uniform Building Code (UBC-97). We compare vertical response spectra calculated using the simplified V/H spectra given in Figure 12 with vertical spectra calculated from Equation (1) and similar spectra developed by applying a constant factor of two-thirds to the UBC-97 horizontal spectrum. However, examination of the effects of vertical ground motion on the response of various structural systems is out of scope of the current study.

The fact that the relationship between the vertical and horizontal response spectra is dependent on source-to-site distance at relatively short distances is recognized in UBC-97. Section 1631.2 of that code states that *"The vertical component of ground motion may be defined by scaling corresponding horizontal accelerations by a factor of two-thirds. Alternative factors may be used when substantiated by site-specific data. Where the Near-Source Factor, N_a, is greater than 1.0, site-specific vertical response spectra shall be used in lieu of the factor of two-thirds."* The Near-Source Factor N_a is specified in Table 16-S of UBC-97 and is greater than 1.0 for the following cases:

- Seismic Source Type A when the closest distance to a known seismic source is < 10 km
- Seismic Source Type B when the closest distance to a known seismic source is < 5 km

For the above cases, according to UBC-97, site-specific vertical response spectra shall be used. Otherwise, the vertical spectrum may be defined by scaling the corresponding horizontal spectrum by a factor of two-thirds. Seismic Source Types A and B are defined in Table 16-U of UBC-97. Seismic Source Type A is a fault that is capable of producing large magnitude events and that has a high rate of seismic activity, defined as a fault having $M \geq 7.0$ and SR (slip rate) $\geq$ 5 mm/yr. Seismic Source Type B is a fault other than Types A and C, where Type C is a fault that is not capable of producing large magnitude earthquakes and that has a relatively low rate of seismic activity (i.e., $M < 6.5$, SR $\leq$ 2 mm/yr). Therefore, Seismic Source Type B is a fault for which either $M \geq 7.0$ and SR < 5 mm/yr, or $M < 7.0$ and SR > 2 mm/yr, or $M \geq 6.5$ and SR < 2 mm/yr.

Figure 13 compares vertical response spectra calculated using three different methods. The first method predicts the vertical spectrum using Equation (1). The second method calculates the vertical spectrum by multiplying the design horizontal response spectrum developed in accordance with Figure 16-3 of UBC-97 by two-thirds. The third method calculates the vertical spectrum by multiplying the simplified V/H spectrum from Figure 12 by the UBC-97 horizontal design spectrum. Compared to the predicted vertical spectrum for Holocene Soil, the two-thirds scaled UBC-97 horizontal spectrum for Soil Profile Type S_D, which is consistent with the Holocene Soil category defined in this study, is generally unconservative around the 0.1-sec spectral peak of the predicted vertical spectrum. It should be noted that structural members may have vertical natural periods in this period range (Bozorgnia and others, 1998). For the other soil

categories, the two-thirds scaled UBC-97 horizontal spectrum might result in more reasonable values. For example, as Figure 13 shows, there is better agreement between the predicted Hard Rock spectrum and the two-thirds scaled UBC-97 horizontal spectrum for Soil Profile Type S_B.

In reviewing similar comparisons between the vertical spectrum predicted from Equation (1) and the vertical spectrum calculated by applying the simplified V/H spectrum to the UBC-97 horizontal design spectrum, we come to the general conclusion that the latter is relatively conservative. The degree of conservatism varies with the type of faulting and the source-to-site distance. This conservatism is probably caused by the inherent conservatism in the UBC-97 horizontal design spectrum and, therefore, might be acceptable. This approach seems to have merit and will be refined in a future study.

CONCLUSIONS AND RECOMMENDATIONS

Based on the results of our study, we offer the following conclusions and recommendations regarding the prediction of the vertical response spectrum and the V/H spectral ratio:

1. The Corrected database is severely limited for small magnitudes ($M_W < 6.0$) at moderate distances and for large magnitudes ($M_W > 7.0$) at all distances, which has resulted in a bias in the attenuation relationships for PGA, SA, and V/H spectral ratio compared to a similar analysis using the Uncorrected database. The Uncorrected database compiled for this study has over two times the number of recordings as the Corrected database. In order to make the regression analysis on Corrected PGA and spectral acceleration more reliable, consideration should be given to extending the accelerogram processing to a wider range of magnitudes and distances.
2. The standard low-pass filter applied during Phase 2 of the accelerogram processing (around 20 to 25 Hz) is not sufficient to capture all of the significant high-frequency energy contained in near-source recordings of vertical ground motion. This is exacerbated by the need to remove those recordings that have low-pass filters less than 25 Hz, which reduced the number of available recordings to the point that the 0.04-sec spectral ordinate became unstable in the regression analysis and could not be used. In order to capture all significant high-frequency energy in near-source vertical recordings, the low-pass filter should be extended to as high a frequency as allowed by the processing noise.
3. An analysis of residuals determined that the estimation of the V/H spectral ratio from attenuation relationships developed independently from the horizontal and vertical components of PGA and SA are unbiased, so that these attenuation relationships can be used to estimate V/H.
4. The V/H spectral ratio is a strong function of oscillator period, source-to-site distance, and local soil conditions, and a weaker function of magnitude and type of faulting. The largest short-period V/H ratios are observed to occur on Holocene Soil at short periods and short distances where they can reach values in excess of 1.5 at 0.1-sec period. The largest long-period V/H ratios are observed to occur on Hard Rock where they can reach values as high as 0.7. Generally V/H is 0.5 or less at the longer periods (0.3 to 2.0 sec).
5. The concept of shifting the horizontal response spectrum to shorter periods and reducing its amplitude to approximate the vertical response spectrum is only valid over a limited range of magnitudes, distances, and soil conditions. In order for this procedure to work for a broader

range of conditions, it will need to be modified to account for differences in these parameters.

6. We conclude that the standard engineering practice of assigning the V/H ratio a value of two-thirds is unconservative at short periods, especially for unconsolidated soil and in the near-source region, but conservative at long periods, and should be modified. Such a modification is recommended in the 1997 Uniform Building Code when the site is located close to a fault, but UBC-97 gives no guidance on how that should be done. We propose a simplified method for estimating a design vertical response spectrum for engineering purposes from a simplified model of V/H that better fits the observed trends in V/H. The procedure seems to have merit and will be refined in a future study.

ACKNOWLEDGEMENTS

This study was supported by the California Department of Conservation, Division of Mines and Geology, Strong Motion Instrumentation Program, Contract 1097-606. The support is gratefully acknowledged.

REFERENCES

Abrahamson, N.A., and J.J. Litehiser (1989). "Attenuation of vertical peak acceleration," *Bulletin of the Seismological Society of America*, Vol. 79, p. 549–580.

Abrahamson, N.A., and W.J. Silva (1997). "Empirical response spectral attenuation relations for shallow crustal earthquakes," *Seismological Research Letters*, Vol. 68, p. 94–127.

Amirbekian, R.V., and B.A. Bolt (1998). "Spectral comparison of vertical and horizontal seismic strong ground motions in alluvial basins," *Earthquake Spectra*, Vol. 14, p. 573–595.

Ansary, M.H., and F. Yamazaki (1998). "Behavior of horizontal and vertical SV at JMA sites, Japan," *Journal of Geotechnical and Geoenvironmental Engineering*, Vol. 124, p. 606–616.

Bozorgnia, Y., and M. Niazi (1993). "Distance scaling of vertical and horizontal response spectra of the Loma Prieta earthquake," *Earthquake Engineering and Structural Dynamics*, Vol. 22, p. 695–707.

Bozorgnia, Y., M. Niazi, and K.W. Campbell (1995). "Characteristics of free-field vertical ground motion during the Northridge earthquake," *Earthquake Spectra*, Vol. 11, p. 515–525.

Bozorgnia, Y., M. Niazi, and K.W. Campbell (1996). "Relationship between vertical and horizontal ground motion for the Northridge earthquake," in *Proceedings, 11th World Conference on Earthquake Engineering*, Acapulco, Mexico.

Bozorgnia, Y., S.A. Mahin, and A.G. Brady (1998). "Vertical response of twelve structures recorded during the Northridge earthquake," *Earthquake Spectra*, Vol. 14, p. 411–432.

Campbell, K.W. (1982). "A Study of the near-source behavior of peak vertical acceleration", (Abs.), *EOS*, Vol. 63, p. 1,037.

Campbell, K.W. (1991). "An empirical analysis of peak horizontal acceleration for the Loma Prieta, California, earthquake of 18 October 1989," *Bulletin of the Seismological Society of America*, Vol. 81, p. 1838–1858.

Campbell, K.W. (1997). "Empirical near-source attenuation relationships for horizontal and vertical components of peak ground acceleration, peak ground velocity, and pseudo-absolute acceleration response spectra," *Seismological Research Letters*, Vol. 68, p. 154–179.

Campbell, K.W., and Y. Bozorgnia (1994). "Near-source attenuation of peak horizontal acceleration From worldwide accelerograms recorded From 1957 to 1993", in *Proceedings, Fifth U.S. National Conference on Earthquake Engineering*, 1993, Chicago, Ill.

Niazi, M., and Y. Bozorgnia (1989). "Behavior of vertical ground motion parameters in the near field," (Abs.), *Seismological Research Letters*, Vol. 60, No. 1.

Niazi, M., and Y. Bozorgnia (1990). "Observed ratios of PGV/PGA and PGD/PGA for deep soil sites across SMART-1 array, Taiwan," in *Proceedings, 4th U.S. National Conference on Earthquake Engineering*, Palm Springs, Calif., Vol. 1, p. 367–374.

Niazi, M., and Y. Bozorgnia (1991). "Behavior of near-source peak vertical and horizontal ground motions over SMART-1 array, Taiwan," *Bulletin of the Seismological Society of America*, Vol. 81, p. 715–732.

Niazi, M., and Y. Bozorgnia (1992). "Behavior of near-source vertical and horizontal response spectra at SMART-1 array, Taiwan," *Earthquake Engineering and Structural Dynamics*, Vol. 21, p. 37–50.

Sadigh, K., C.-Y. Chang, N.A. Abrahamson, S.J. Chiou, and M.S. Power (1993). "Specification of long-period ground motions: updated attenuation relationships for rock site conditions and adjustment factors for near-fault effects," in *Proceedings, ATC-17-1 Seminar on Seismic Isolation, Passive Energy Dissipation, and Active Control*, San Francisco, Calif., Applied Technology Council Report ATC-17-1, Vol. 1, p. 59–70.

Somerville, P., and J. Yoshimura (1990). "The influence of critical MOHO reflections on strong ground motions recorded in San Francisco and Oakland during the 1989 Loma Prieta earthquake," *Geophysical Research Letters*, Vol. 17, p. 1203–1206.

Uniform Building Code (1997). International Conference of Building Officials, Whittier, CA, Volume 2.

Watabe, M., M. Tohido, O. Chiba, and R. Fukuzawa (1990). "Peak accelerations and response spectra of vertical strong motions from near-field records in USA," in *Proceedings, 8th Japan Earthquake Engineering Symposium*, Vol. 1, p. 301–306.

Table 1—Earthquakes Used in the Current Study

Earthquake	Location	Corrected	Year	M_W	Type of Faulting
Daly City	California	Yes	1957	5.3	Reverse Oblique
Parkfield	California	Yes	1966	6.1	Strike Slip
Koyna	India	Yes	1967	6.3	Strike Slip
Lytle Creek	California	Yes	1970	5.3	Reverse
San Fernando	California	Yes	1971	6.6	Reverse
Sitka	Alaska	Yes	1972	7.7	Strike Slip
Stone Canyon	California	Yes	1972	4.7	Strike Slip
Managua	Nicaragua	Yes	1972	6.2	Strike Slip
Point Magu	California	No	1973	5.6	Reverse
Hollister	California	Yes	1974	5.1	Strike Slip
Oroville	California	Yes	1975	6.0	Normal
Kalapana	Hawaii	No	1975	7.1	Thrust
Gazli	Uzbekistan	Yes	1976	6.8	Reverse
Caldiran	Turkey	Yes	1976	7.3	Strike Slip
Mesa de Andrade	Mexico	No	1976	5.6	Strike Slip
Santa Barbara	California	Yes	1978	6.0	Thrust
Tabas	Iran	Yes	1978	7.4	Thrust
Bishop	California	No	1978	5.8	Strike Slip
Malibu	California	No	1979	5.0	Reverse
St. Elias	Alaska	No	1979	7.6	Thrust
Coyote Lake	California	Yes	1979	5.8	Strike Slip
Imperial Valley	California	Yes	1979	6.5	Strike Slip
Livermore	California	No	1980	5.8	Strike Slip
Livermore Aftershock	California	No	1980	5.4	Strike Slip
Westmorland	California	No	1981	6.0	Strike Slip
Morgan Hill	California	Yes	1984	6.2	Strike Slip
Nahanni	Canada	Yes	1985	6.8	Thrust
North Palm Springs	California	Yes	1986	6.1	Strike Slip
Chalfant Valley	California	No	1986	6.3	Strike Slip
Whittier Narrows	California	Yes	1987	6.1	Thrust
Whittier Narrows Aftershock	California	Yes	1987	5.3	Reverse Oblique
Elmore Ranch	California	Yes	1987	6.2	Strike Slip
Superstition Hills	California	Yes	1987	6.6	Strike Slip
Spitak	Armenia	Yes	1988	6.8	Reverse Oblique
Pasadena	California	No	1988	5.0	Strike Slip
Loma Prieta	California	Yes	1989	6.9	Reverse Oblique
Malibu	California	No	1989	5.0	Thrust
Manjil	Iran	Yes	1990	7.4	Strike Slip
Upland	California	Yes	1990	5.6	Strike Slip
Sierra Madre	California	Yes	1991	5.6	Reverse
Landers	California	Yes	1992	7.4	Strike Slip
Big Bear	California	Yes	1992	6.6	Strike Slip
Joshua Tree	California	No	1992	6.2	Strike Slip
Petrolia	California	Yes	1992	7.1	Thrust
Petrolia Aftershock	California	No	1992	7.0	Strike Slip
Erzincan	Turkey	Yes	1992	6.7	Strike Slip
Northridge	California	Yes	1994	6.7	Thrust
Kobe	Japan	Yes	1995	6.9	Strike Slip

Table 2—Results of Regression Analysis of Horizontal and Vertical Components of PGA and SA

Period (sec)	c_1	c_2	c_3	c_4	c_5	c_6	c_7	c_8	c_9	c_{10}	c_{11}	c_{12}	c_{13}	c_{14}	c_{15}	c_{16}	No.	σ	r^2
Mean Horizontal Component																			
Unc PGA	-2.896	0.812	0.000	-1.318	0.187	-0.029	-0.064	0.616	0.000	0	0.179	0.307	0	-0.062	-0.195	-0.320	960	0.509	0.955
Cor PGA	-4.033	0.812	0.036	-1.061	0.041	-0.005	-0.018	0.766	0.034	0	0.343	0.351	0	-0.123	-0.138	-0.289	443	0.465	0.949
0.05	-3.740	0.812	0.036	-1.121	0.054	0.000	-0.024	0.724	0.032	0	0.302	0.362	0	-0.140	-0.158	-0.205	435	0.485	0.940
0.075	-3.076	0.812	0.050	-1.252	0.121	-0.005	-0.035	0.648	0.040	0	0.243	0.333	0	-0.150	-0.196	-0.208	439	0.497	0.923
0.10	-2.661	0.812	0.060	-1.308	0.166	-0.009	-0.052	0.621	0.046	0	0.224	0.313	0	-0.146	-0.253	-0.258	439	0.503	0.901
0.15	-2.270	0.812	0.041	-1.324	0.212	-0.033	-0.044	0.613	0.031	0	0.318	0.344	0	-0.176	-0.267	-0.284	439	0.519	0.862
0.20	-2.771	0.812	0.030	-1.153	0.098	-0.012	-0.020	0.704	0.026	0	0.296	0.342	0	-0.148	-0.183	-0.359	439	0.526	0.844
0.30	-2.999	0.812	0.007	-1.080	0.064	-0.010	-0.027	0.752	0.007	0	0.359	0.385	0	-0.162	-0.157	-0.585	439	0.512	0.859
0.40	-3.511	0.812	-0.015	-0.964	0.019	0	0	0.842	-0.016	0	0.379	0.438	0	-0.078	-0.129	-0.557	439	0.532	0.871
0.50	-3.556	0.812	-0.035	-0.964	0.019	0	0	0.842	-0.036	0	0.406	0.479	0	-0.122	-0.130	-0.701	439	0.535	0.890
0.75	-3.709	0.812	-0.071	-0.964	0.019	0	0	0.842	-0.074	0	0.347	0.419	0	-0.108	-0.124	-0.796	438	0.566	0.917
1.0	-3.867	0.812	-0.101	-0.964	0.019	0	0	0.842	-0.105	0	0.329	0.338	0	-0.073	-0.072	-0.858	438	0.582	0.935
1.5	-4.093	0.812	-0.150	-0.964	0.019	0	0	0.842	-0.155	0	0.217	0.188	0	-0.079	-0.056	-0.954	428	0.557	0.960
2.0	-4.311	0.812	-0.180	-0.964	0.019	0	0	0.842	-0.187	0	0.060	0.064	0	-0.124	-0.116	-0.916	405	0.543	0.971
3.0	-4.817	0.812	-0.193	-0.964	0.019	0	0	0.842	-0.200	0	-0.079	0.021	0	-0.154	-0.117	-0.873	333	0.561	0.976
4.0	-5.211	0.812	-0.202	-0.964	0.019	0	0	0.842	-0.209	0	-0.061	0.057	0	-0.054	-0.261	-0.889	275	0.579	0.978
Vertical Component																			
Unc PGA	-2.807	0.756	0	-1.391	0.191	0.044	-0.014	0.544	0	0	0.091	0.223	0	-0.096	-0.212	-0.199	941	0.548	0.964
Cor PGA	-3.108	0.756	0	-1.287	0.142	0.046	-0.040	0.587	0	0	0.253	0.173	0	-0.135	-0.138	-0.256	439	0.520	0.958
0.05	-1.918	0.756	0	-1.517	0.309	0.069	0.010	0.498	0	0	0.058	0.100	0	-0.195	-0.274	-0.219	434	0.592	0.934
0.075	-1.504	0.756	0	-1.551	0.343	0.115	0.067	0.487	0	0	0.135	0.182	0	-0.224	-0.303	-0.263	436	0.602	0.910
0.10	-1.672	0.756	0	-1.473	0.282	0.062	0.001	0.513	0	0	0.168	0.210	0	-0.198	-0.275	-0.252	436	0.591	0.900
0.15	-2.323	0.756	0	-1.280	0.171	0.045	0.008	0.591	0	0	0.223	0.238	0	-0.170	-0.175	-0.270	436	0.574	0.899
0.20	-2.998	0.756	0	-1.131	0.089	0	-0.013	0.668	0	0	0.234	0.256	0	-0.098	-0.041	-0.311	436	0.551	0.915
0.30	-3.721	0.756	0.007	-1.028	0.050	0	-0.007	0.736	0.007	0	0.249	0.328	0	-0.026	0.082	-0.265	436	0.509	0.941
0.40	-4.536	0.756	-0.015	-0.812	0.012	0	0	0.931	-0.018	0	0.299	0.317	0	-0.017	0.022	-0.257	436	0.521	0.949
0.50	-4.651	0.756	-0.035	-0.812	0.012	0	0	0.931	-0.043	0	0.243	0.354	0	-0.020	0.092	-0.293	436	0.515	0.957
0.75	-4.903	0.756	-0.071	-0.812	0.012	0	0	0.931	-0.087	0	0.295	0.418	0	0.078	0.091	-0.349	435	0.556	0.962
1.0	-4.950	0.756	-0.101	-0.812	0.012	0	0	0.931	-0.124	0	0.266	0.315	0	0.043	0.101	-0.481	435	0.562	0.967
1.5	-5.073	0.756	-0.150	-0.812	0.012	0	0	0.931	-0.184	0	0.171	0.211	0	-0.038	-0.018	-0.518	420	0.581	0.973
2.0	-5.292	0.756	-0.180	-0.812	0.012	0	0	0.931	-0.222	0	0.114	0.115	0	0.033	-0.022	-0.503	395	0.591	0.977
3.0	-5.748	0.756	-0.193	-0.812	0.012	0	0	0.931	-0.238	0	0.179	0.159	0	-0.010	-0.047	-0.539	321	0.617	0.978
4.0	-6.042	0.756	-0.202	-0.812	0.012	0	0	0.931	-0.248	0	0.237	0.134	0	-0.059	-0.267	-0.606	274	0.636	0.980

Table 3—Statistical Summary of Predicted V/H

Period (sec)	No.	Bias (ln V/H)	Bias (Factor)	σ
Unc PGA	941	-0.0121	0.99	0.432
Cor PGA	439	-0.0074	0.99	0.422
0.05	432	0.0003	1.00	0.465
0.075	436	-0.0081	0.99	0.470
0.10	436	-0.0098	0.99	0.469
0.15	436	-0.0110	0.99	0.493
0.20	436	-0.0100	0.99	0.480
0.30	436	-0.0094	0.99	0.463
0.40	436	-0.0074	1.00	0.483
0.50	436	-0.0044	1.00	0.491
0.75	435	-0.0057	0.99	0.487
1.0	435	-0.0033	1.00	0.514
1.5	419	-0.0183	0.98	0.487
2.0	393	-0.0292	0.97	0.454
3.0	313	-0.0370	0.96	0.437
4.0	262	0.0055	1.01	0.451

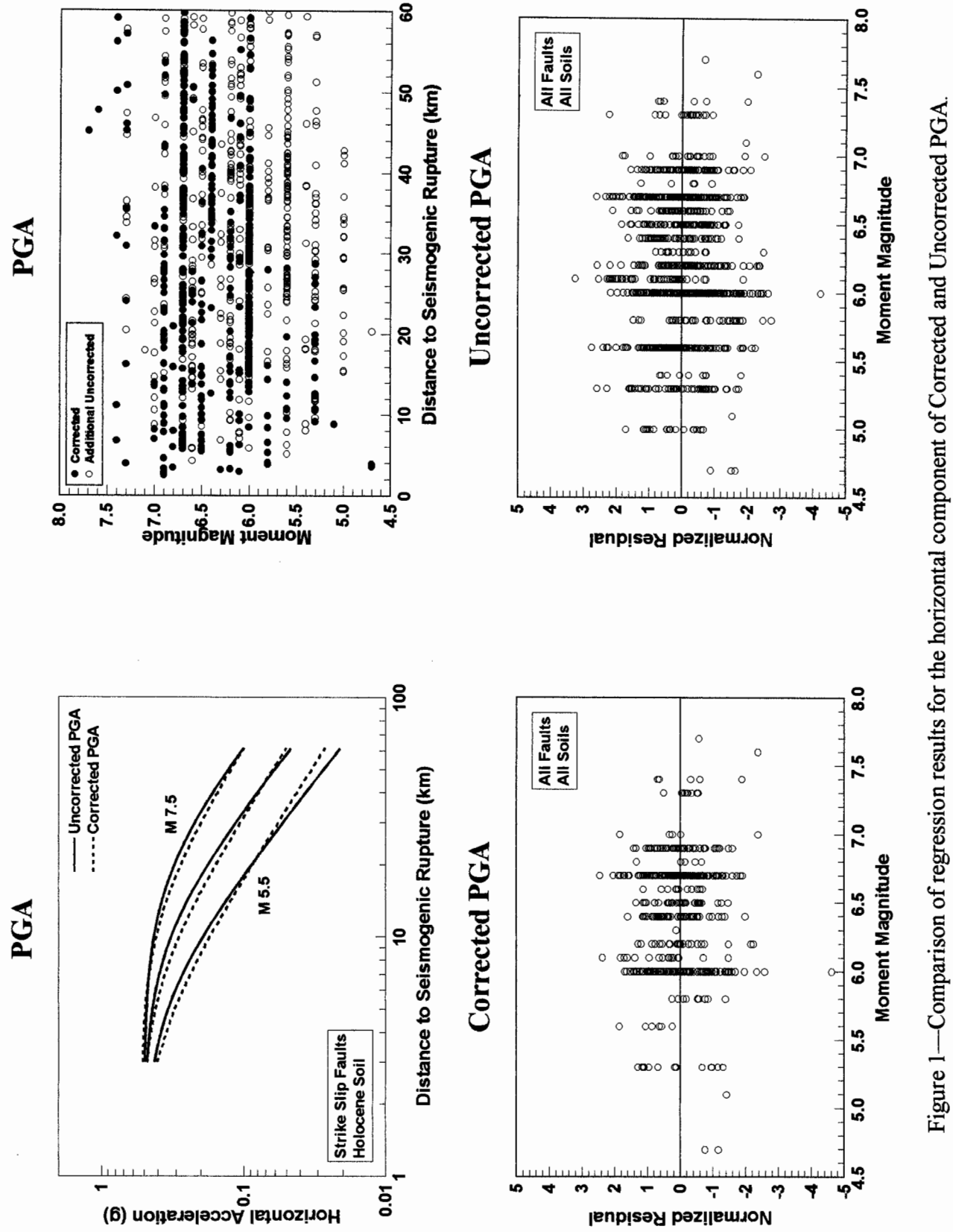

Figure 1—Comparison of regression results for the horizontal component of Corrected and Uncorrected PGA.

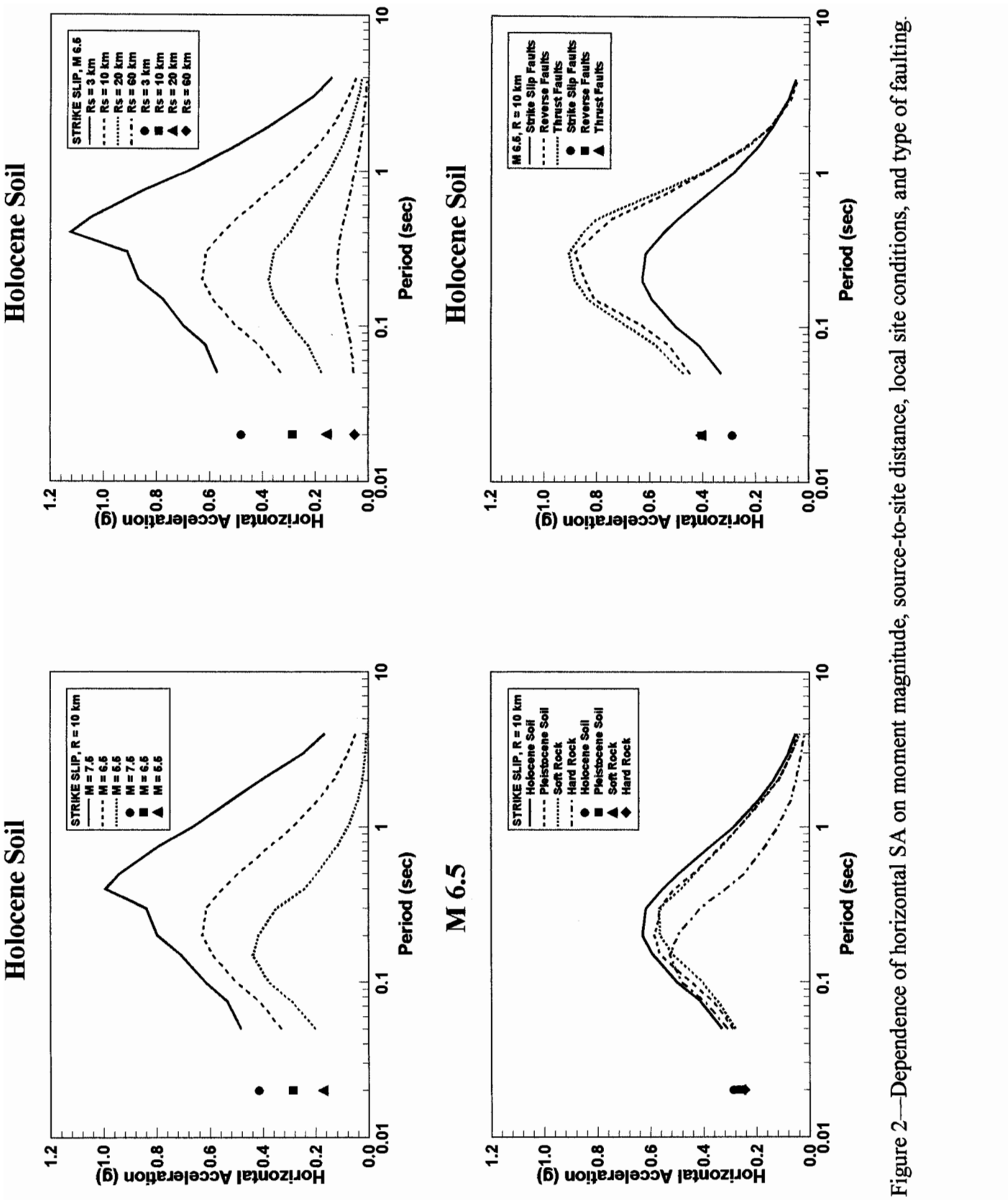

Figure 2—Dependence of horizontal SA on moment magnitude, source-to-site distance, local site conditions, and type of faulting.

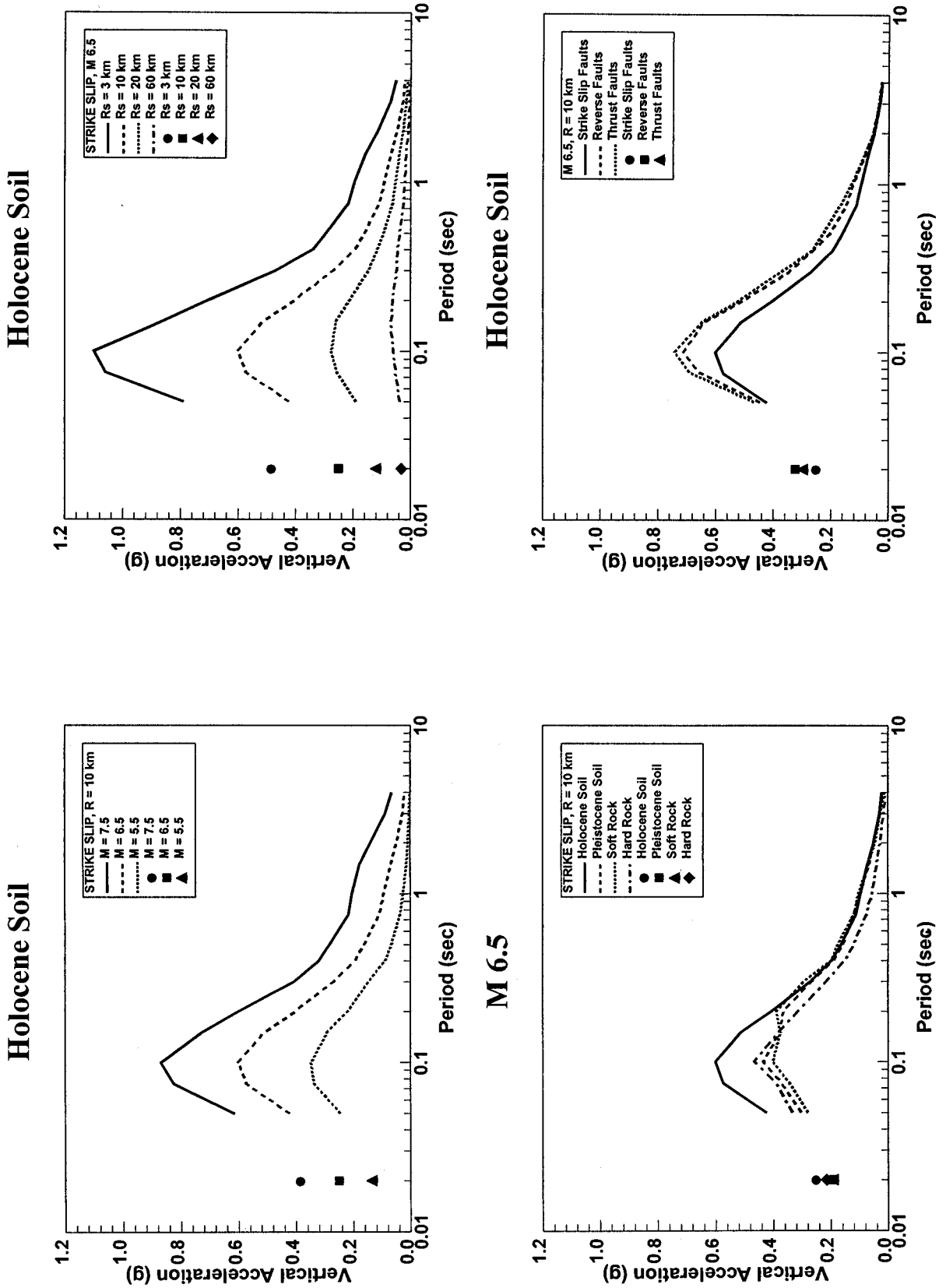

Figure 3—Dependence of vertical SA on moment magnitude, source-to-site distance, local site conditions, and type of faulting.

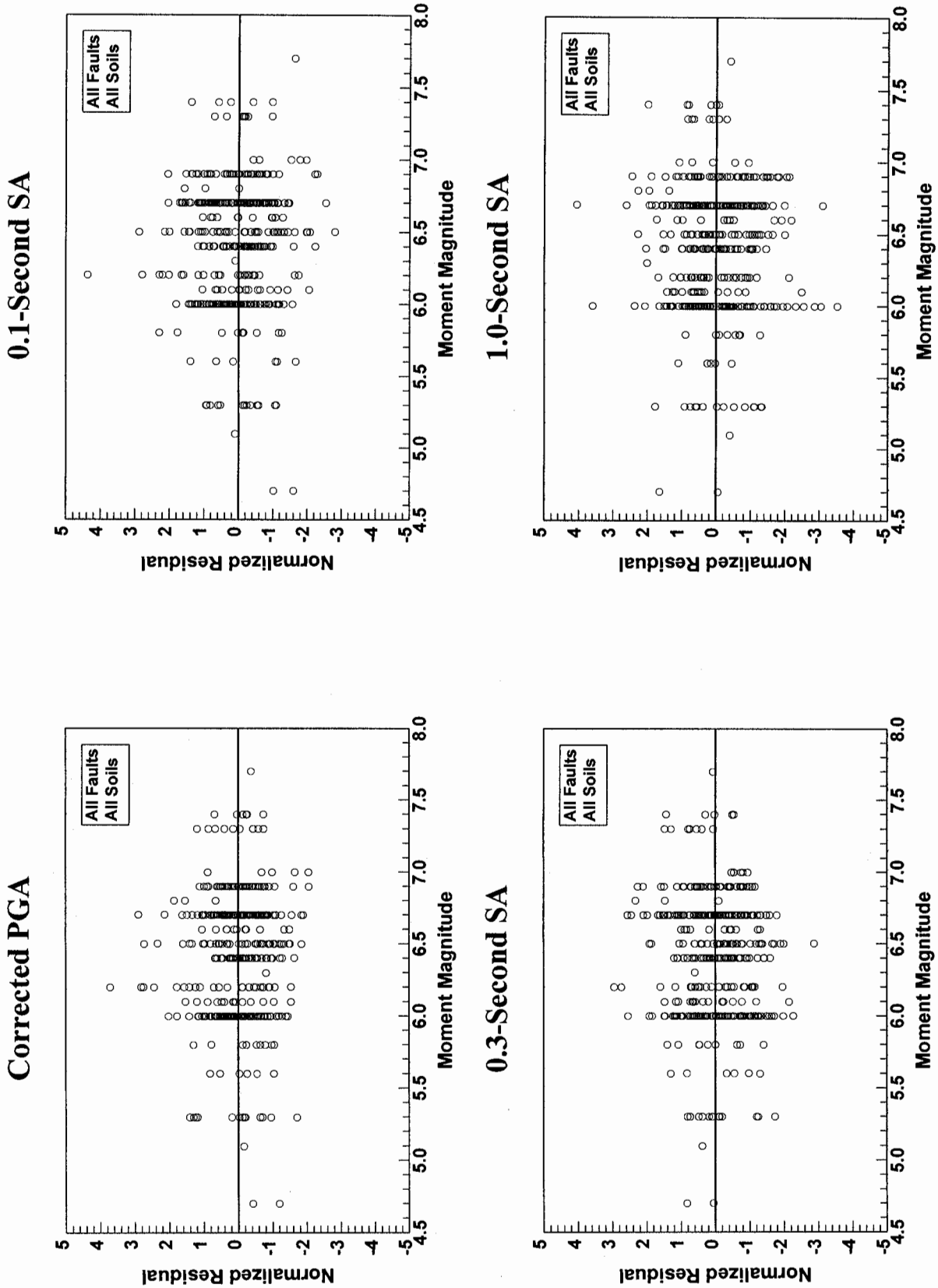

Figure 4—Normalized residuals of V/H versus moment magnitude.

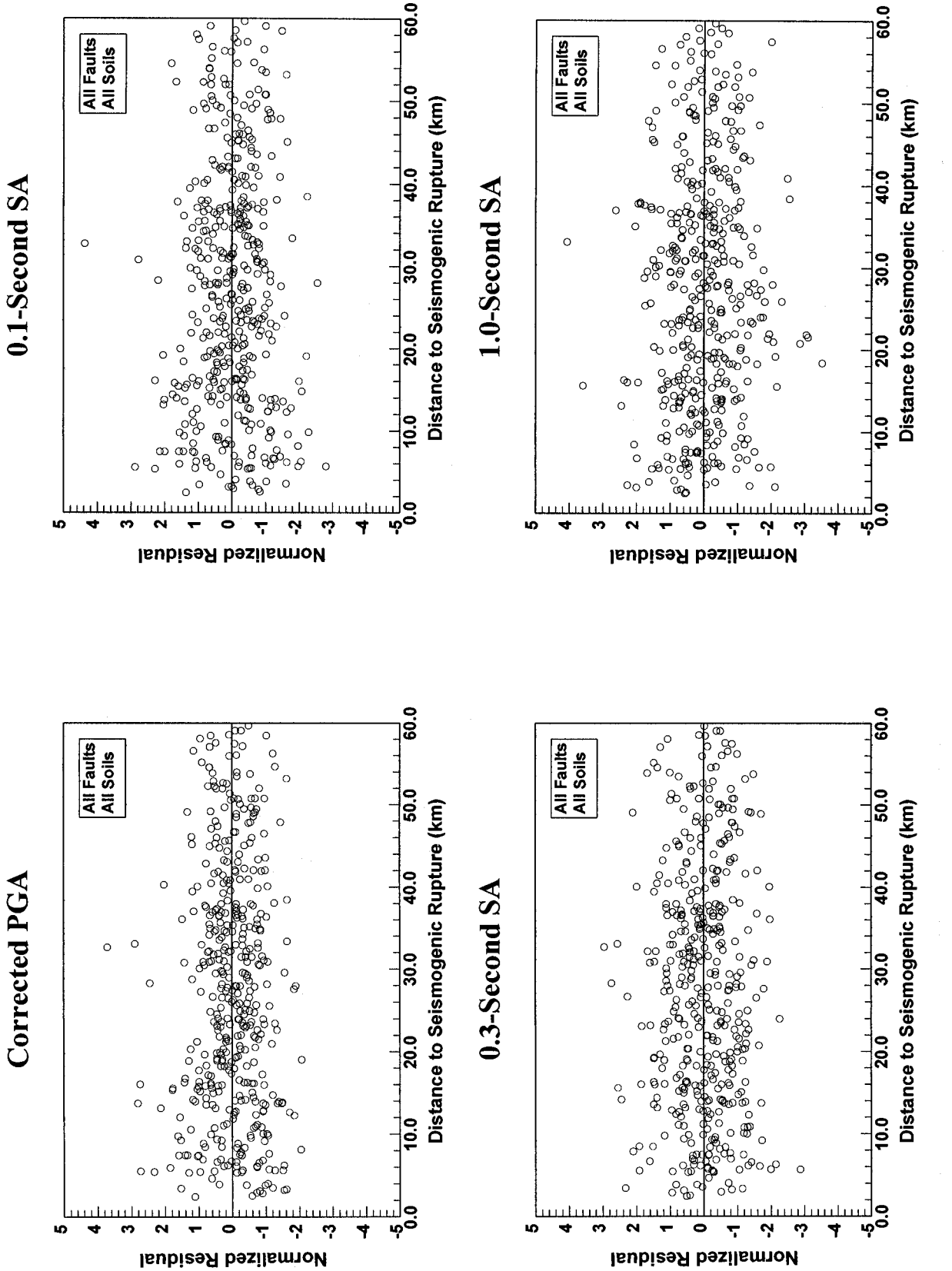

Figure 5—Normalized residuals of V/H versus source-to-site distance.

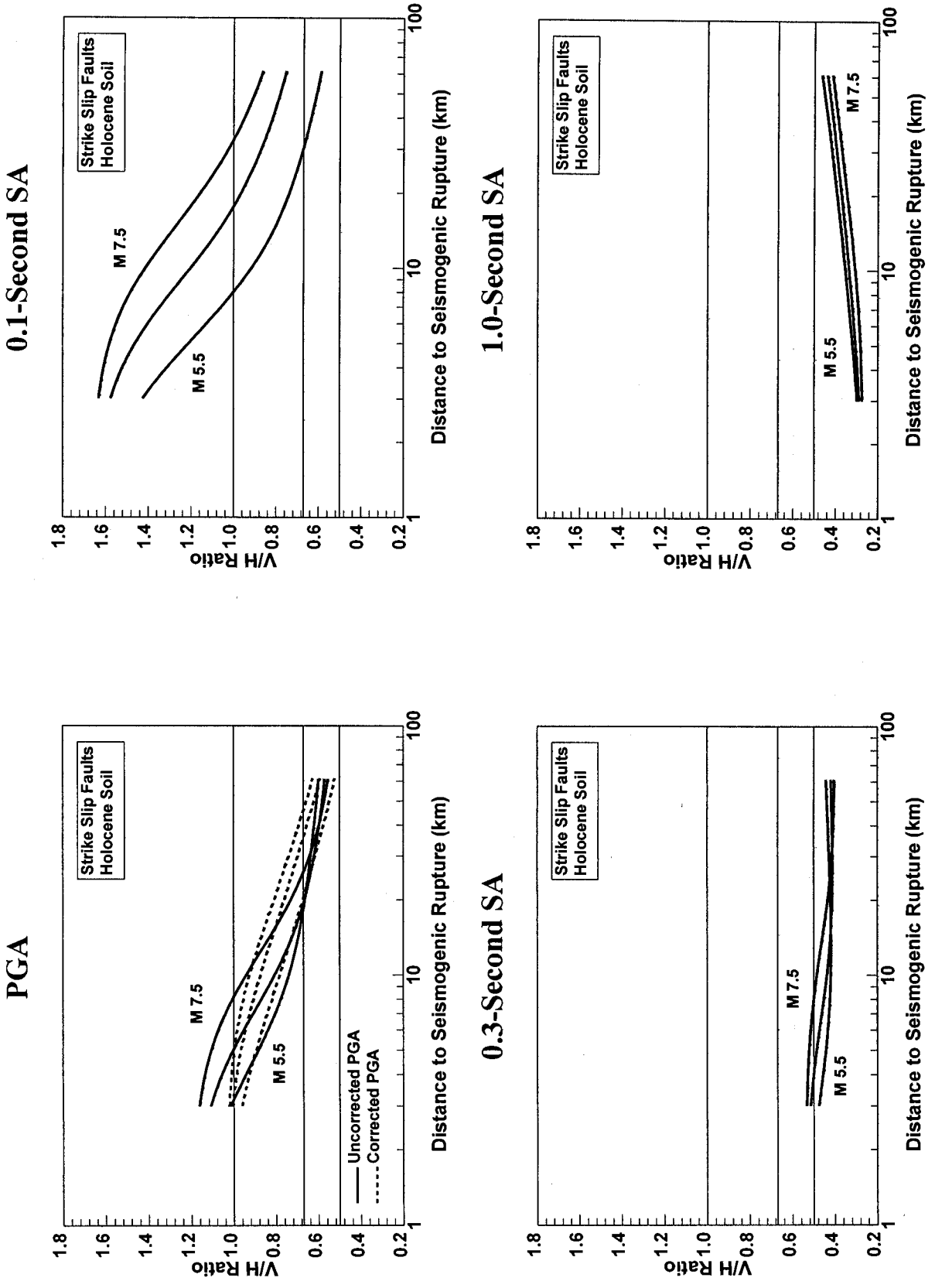

Figure 6—Behavior of V/H spectral ordinates with source-to-site-distance.

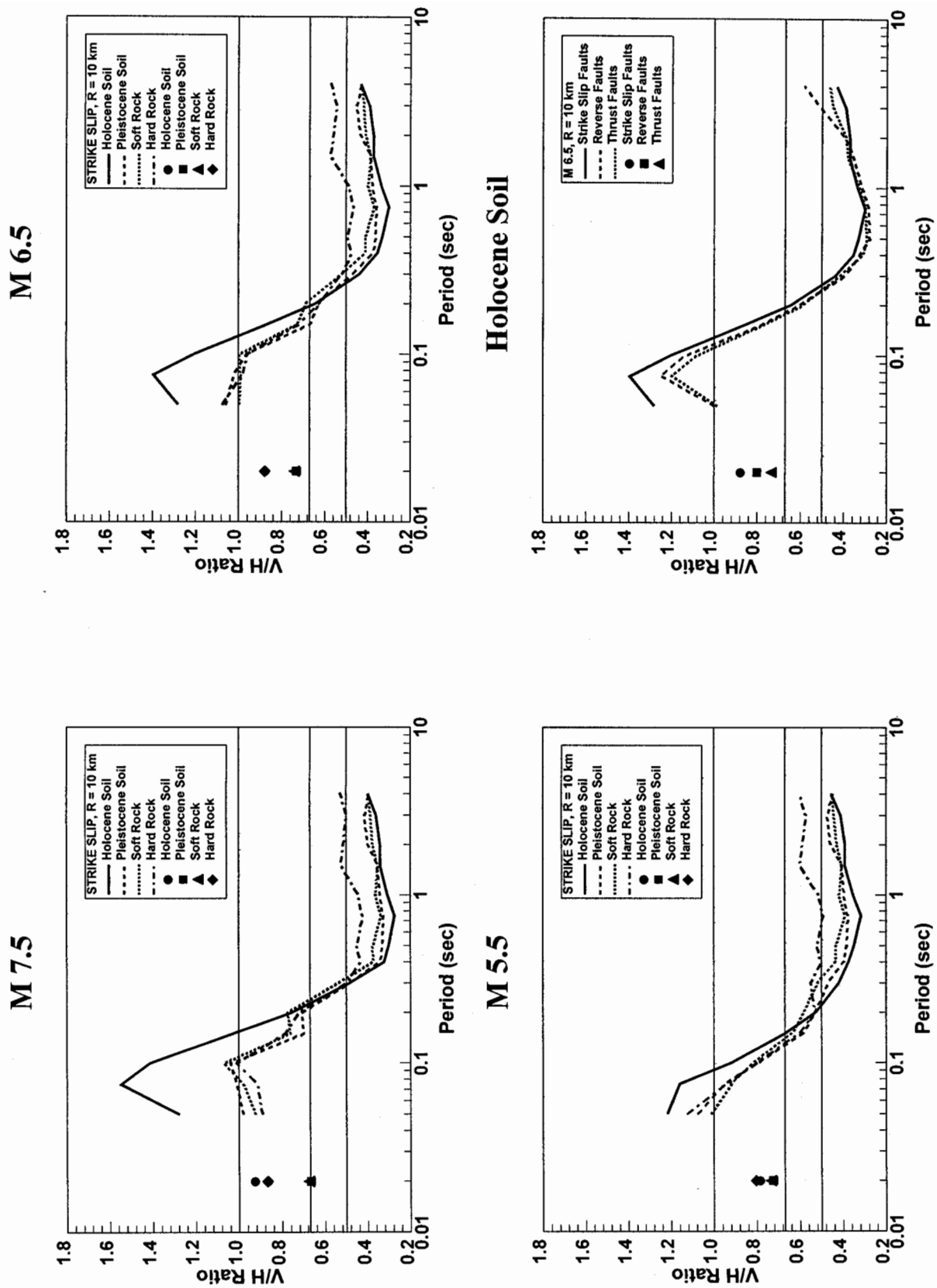

Figure 7—Behavior of V/H spectral ratio with moment magnitude, local soil conditions, and type of faulting.

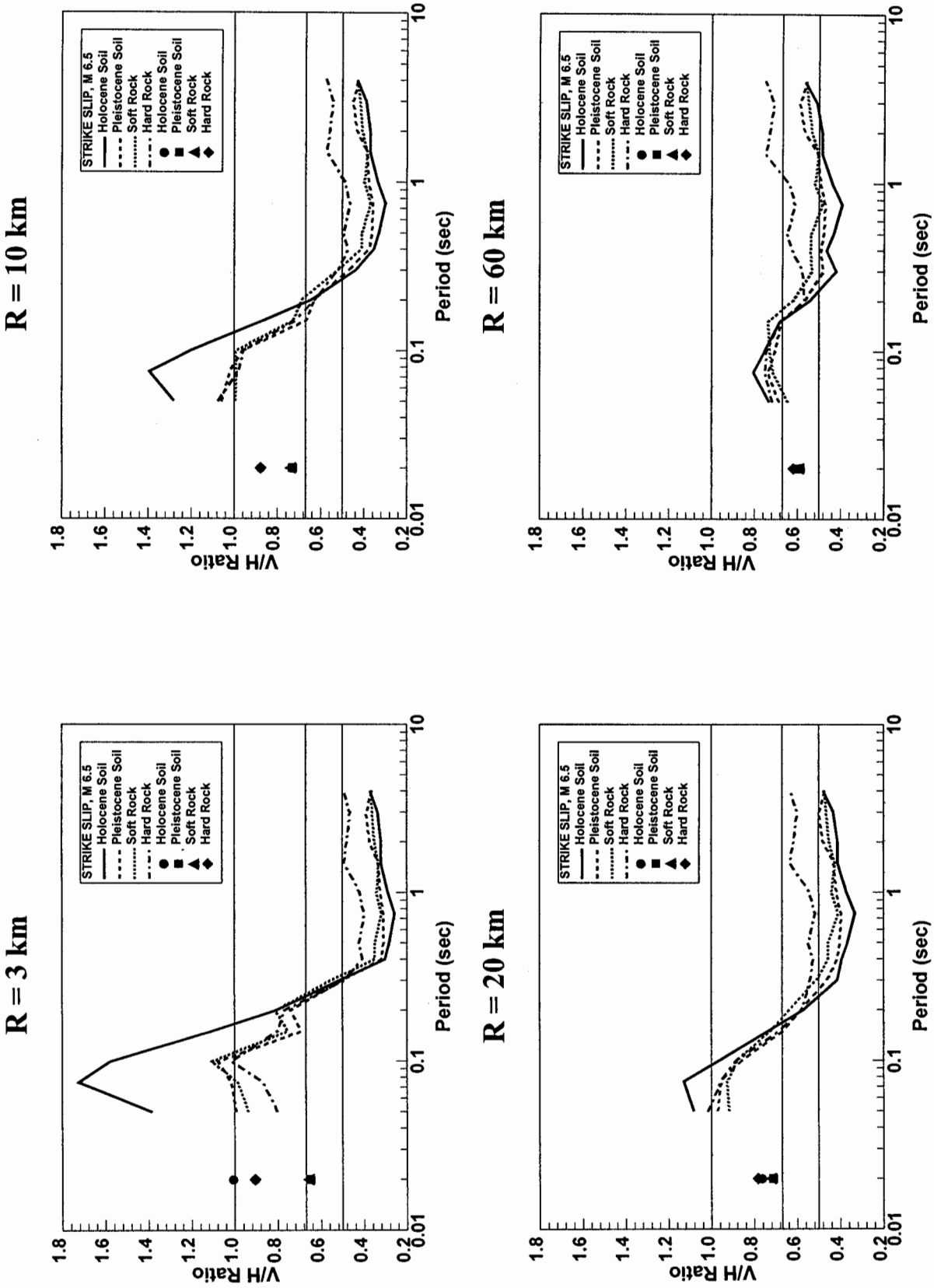

Figure 8—Behavior of V/H spectral ratio with source-to-site distance and local soil conditions.

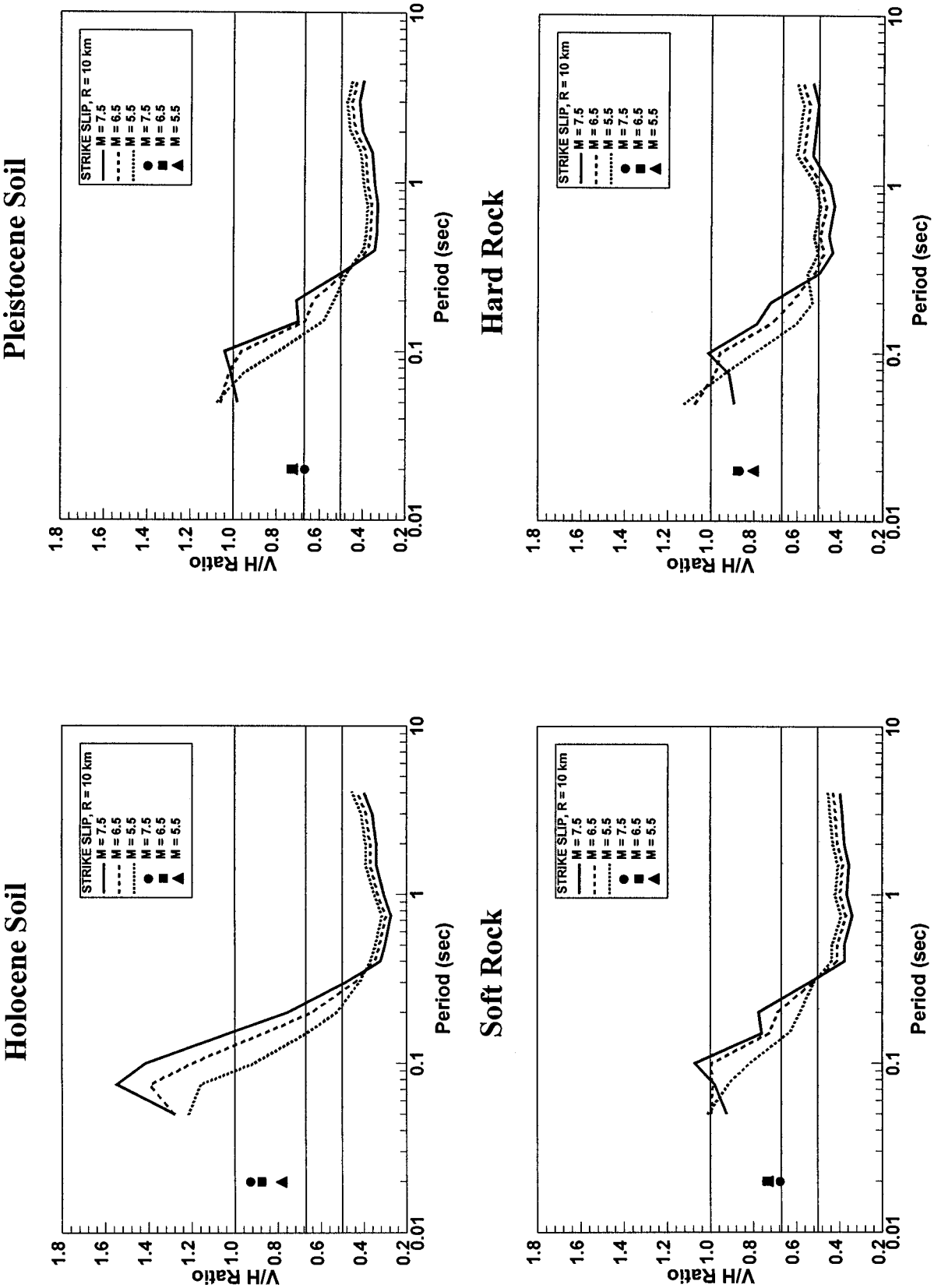

Figure 9—Behavior of V/H spectral ratio with local soil conditions and moment magnitude.

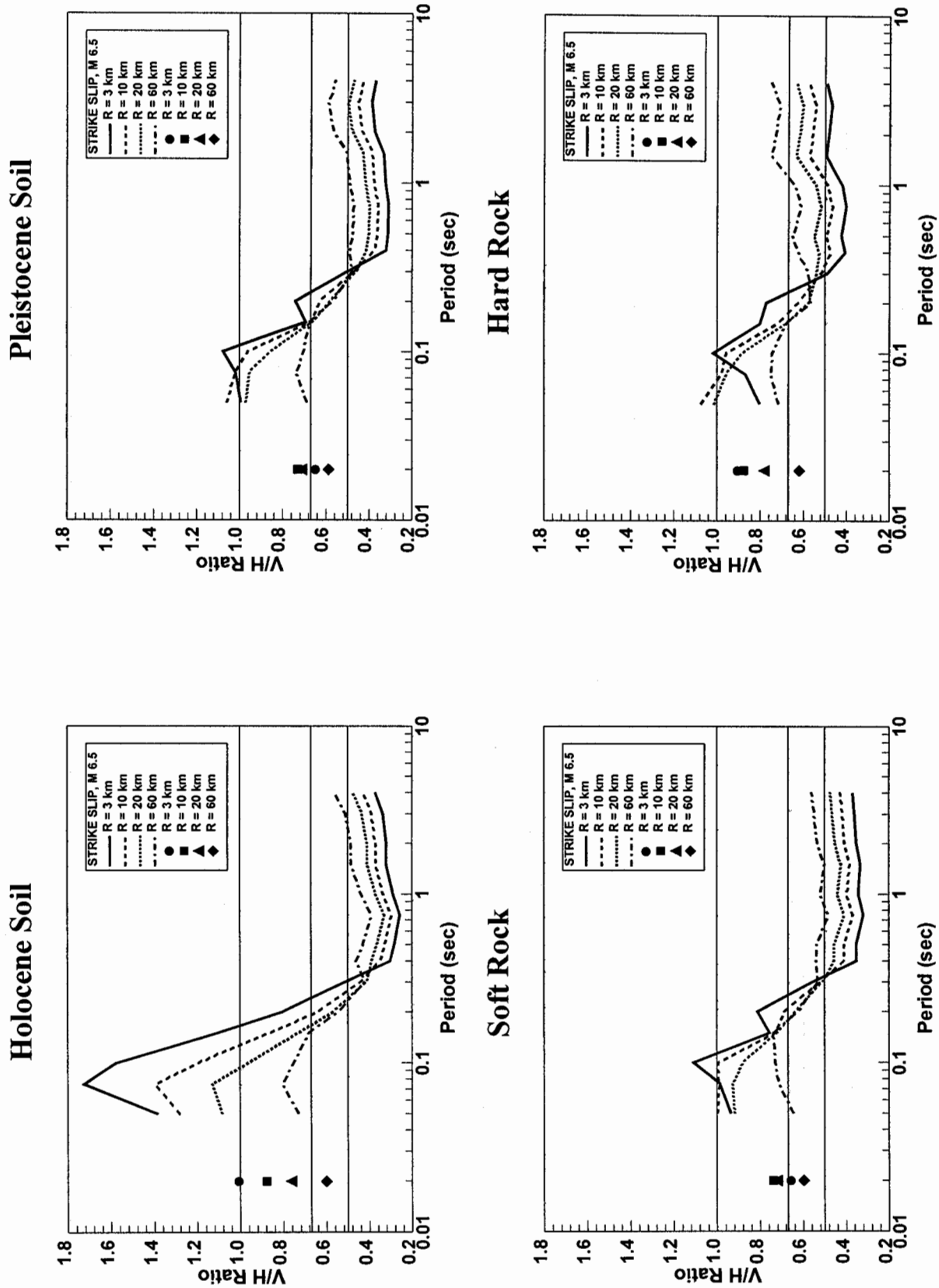

Figure 10—Behavior of V/H spectral ratio with local soil conditions and source-to-site distance.

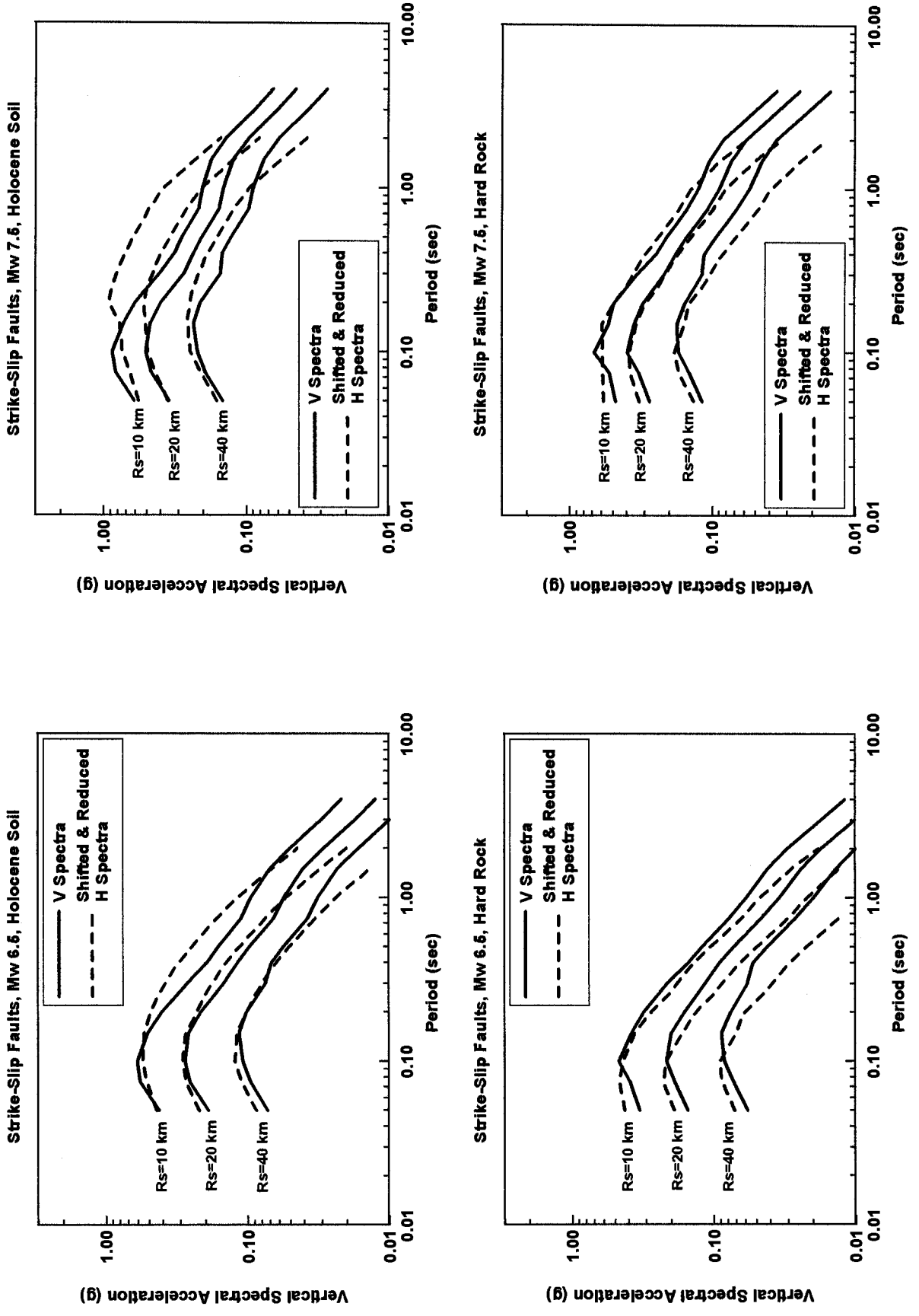

Figure 11—Vertical response spectra and shifted & reduced horizontal spectra.

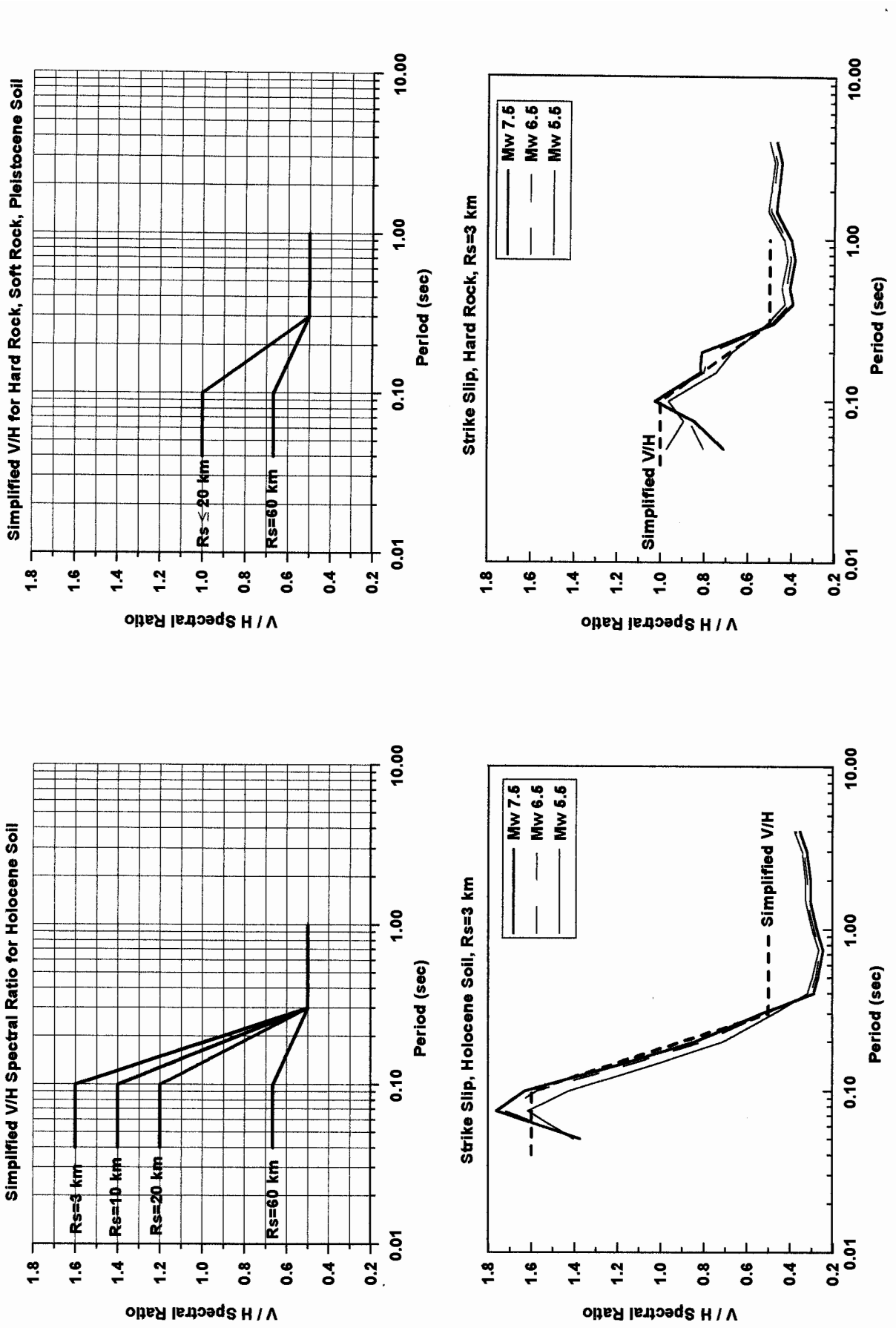

Figure 12—Predicted and simplified V/H spectral ratios.

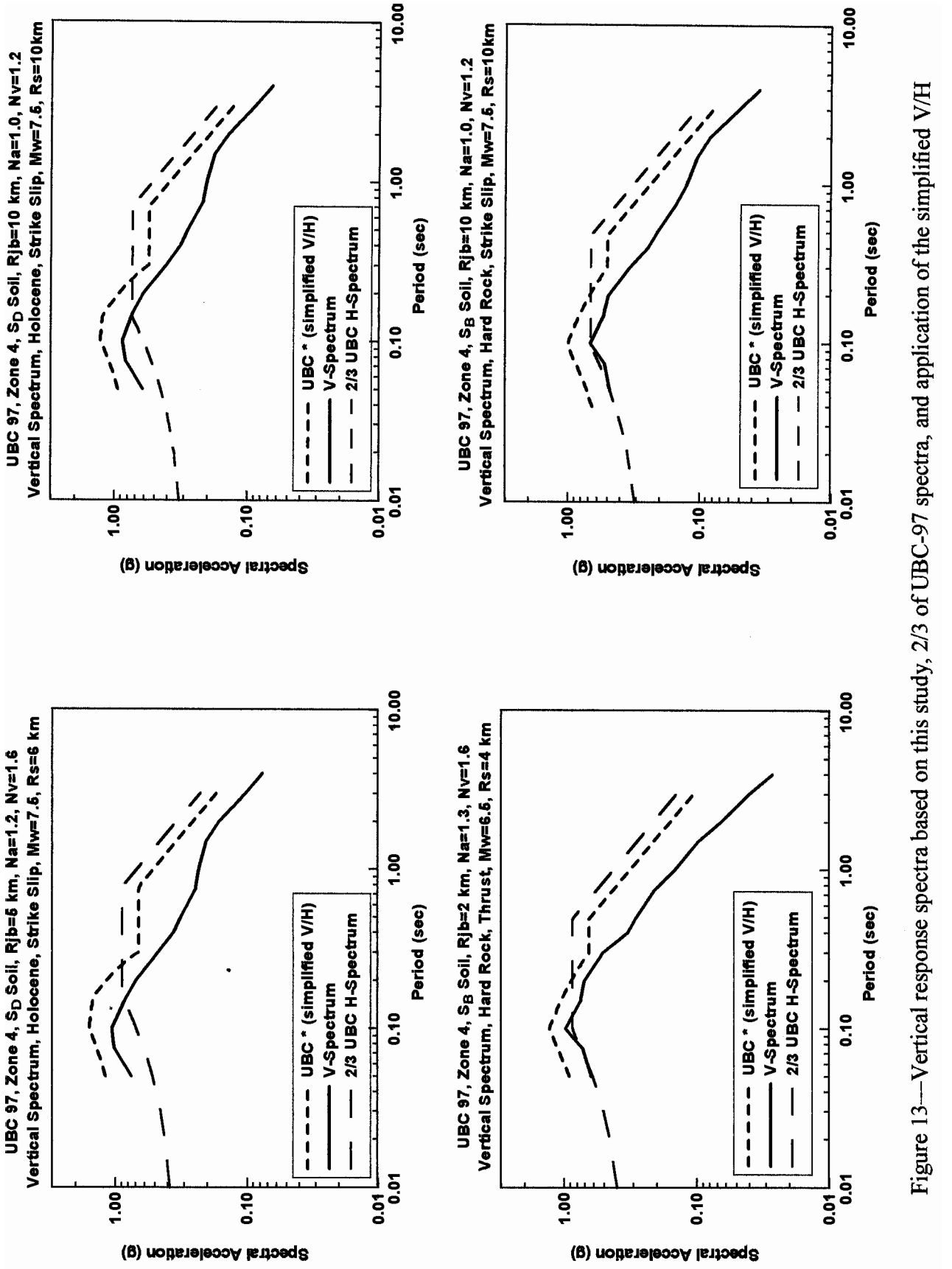

Figure 13—Vertical response spectra based on this study, 2/3 of UBC-97 spectra, and application of the simplified V/H